Supplementary Information

S1. Calculation of age range of rings in a culture going through the schizont-ring transition (Fig. 2A)

A culture of 3D7 parasites consisting of late trophozoites/early schizonts was monitored for the appearance of the next generation of rings by flow cytometry (Fig. S1). The same culture was subjected to 4 h drug pulses every 3 h beginning at the late trophozoite stage and continuing into the next parasite cycle. We correlated the measured LD_{50}(4h) in each assay with the age distribution of rings during the course of each assay. In this approach, one trophozoite/schizont is assumed equivalent to six rings (the amplification achieved in the control culture) and parasites with negative ages, *a*, correspond to trophozoites/schizonts that will form new rings in *a* hours time.

We first fitted an empirical sigmoidal model to the data shown in Fig. S1:

$$R(t) = \left(1 + 10^{k(t)}\right)^{-1} \qquad [S1.1]$$

where *R(t)* is the fraction of the total rings formed that are present at time *t* (with *t = 0* corresponding to the time at which 50% of rings have formed) and *k* the skewness of the curve.

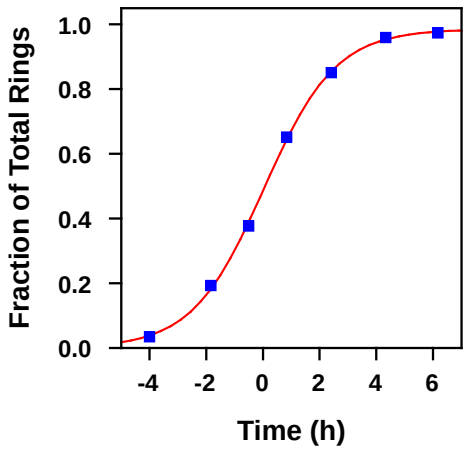

Fig. S1. Time dependence of ring formation in the culture used in Fig. 2A. A culture of 3D7 parasites consisting of late trophozoites/early schizonts was monitored by flow cytometry at different times for the appearance of the next generation of rings (symbols). The curve corresponds to the best fit with Eq. S1.1. Zero time corresponds to the time at which 50% of the rings have formed.

The instantaneous rate of appearance of rings is given by $\dot{R} \equiv dR(t)/dt$, and so the probability density function for rings of age a at time t is $\dot{R}(t-a)$. During the course of an assay running from start time t_s to end time t_e, the time-averaged probably density of rings of age a is given by:

$$\begin{aligned}\hat{p}(a) &= \frac{1}{[t_e - t_s]} \int_{t=t_s}^{t=t_e} \dot{R}(t-a)dt \\ &= \frac{1}{[t_e - t_s]} R(t)\Big|_{t=t_s-a}^{t=t_e-a} \\ &= \frac{1}{[t_e - t_s]} \left[(1+10^{-k(t_e-a)})^{-1} + (1+10^{-k(t_s-a)})^{-1} \right]\end{aligned} \qquad \text{[S1.2]}$$

The LD_{50}(4h) measured in a particular assay will reflect the LD_{50}(4h) of the predominant parasite population in the culture. Thus, for each assay, we calculated the inter-quartile range of the time-averaged probability density of the age of the parasites (Eq. S1.2).

S2a. Derivation of the cumulative effective dose (ED) model for parasite viability

We sought to develop a simple model that could account for the complex dependence of parasite viability (V) on drug concentration (C) and drug exposure time (t^e) (left panels in Fig. S2).

The presence of a lag time in many of the V-t^e relationships (Fig. 3B) indicates that both C and t^e (*i.e.* the cumulative drug dose, D^{cum}) are important determinants of drug susceptibility. However, a simple definition of D^{cum} in terms of the product, Ct^e, produced V-D^{cum} profiles that remained dependant on t^e. We thus distinguished between the actual drug concentration administered to the culture (C) and the effective dose (ED) experienced by the parasite. This effective dose arises from the interaction of the drug with the parasite to produce a product or affect a biological process that is ultimately responsible for parasite death. Parasite viability (V) is therefore a function of the cumulative ED ($ED^{cum} = EDt^e$) while the ED itself is a function of the administered drug concentration. To account for the observation that drug action is almost independent of C at high drug concentrations (e.g. see Fig. 3A), we defined ED in terms of a process exhibiting saturation effects:

$$ED(C) = ED^{max}\left(\frac{C}{K_m + C}\right) \qquad [S2.1]$$

where ED^{max} represents the maximum ED achieved at saturating drug concentration, and K_m the drug concentration producing 50% ED^{max}. If the correct form of ED has been defined, then the relationship between V and the ED^{cum} will be independent of t^e. Our data satisfied this criterion (Fig. S2, right panels) justifying the form of ED selected. The relationship between V and ED^{cum} can then be deduced from the form of the V-ED^{cum} profile. In the case of the artemisinins, this corresponds to a sigmoidal relationship (Fig. S2, right panels) so that:

$$V(ED^{cum}) = 1 - \frac{\left(ED^{cum}\right)^{\gamma}}{\left(ED^{cum}\right)^{\gamma} + \left(ED_{50}^{cum}\right)^{\gamma}} \qquad [S2.2]$$

where γ is the slope of the function and ED_{50}^{cum} the cumulative ED required to kill 50% of the parasites. Substituting $ED^{cum} = EDt^e$ with the definition of ED defined in Eq. S2.1 into Eq. S2.2:

$$V(C,t^e)=\left[1+\left(\frac{ED^{max}Ct^e}{ED_{50}^{cum}\left(K_m+C\right)}\right)^{\gamma}\right]^{-1} \quad \text{[S2.3]}$$

In practice, ED_{50}^{cum} and ED^{max} can only be determined as a ratio:

$$V(C,t^e)=\left[1+\left(\frac{Ct^e}{t_{50}^{e,sat}\left(K_m+C\right)}\right)^{\gamma}\right]^{-1} \quad \text{[S2.4]}$$

where $t_{50}^{e,sat} = ED_{50}^{cum} / ED^{max}$ is the minimum time required to kill 50% of the parasites (at saturating drug concentrations).

Model parameters obtained from the analysis of the 3D7 strain at different parasite stages are summarized in Table 1 (main text).

S2b. Stage-dependance of 3D7 parasite viability on drug concentration and drug exposure time and analysis according to the cumulative effective dose model

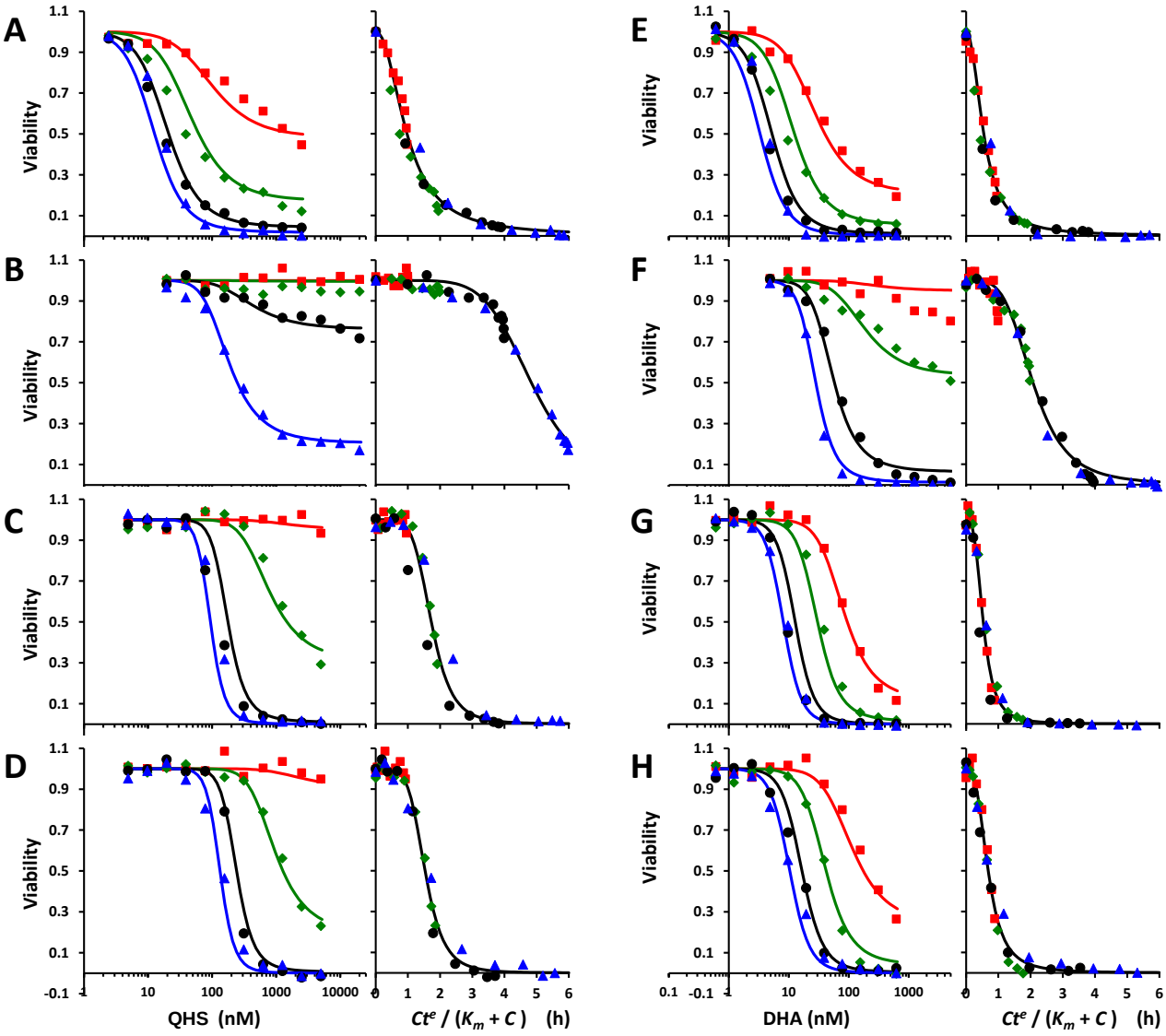

Fig. S2. Dependence of parasite viability on drug concentration, drug exposure time and the cumulative effective dose (3D7 strain). Tightly synchronized parasite cultures (3D7 strain) consisting of hRings (A,E), rings (B,F), early trophozoites (C,G) and late trophozoites (D,H) were exposed to QHS (A-D) or DHA (E-H) for 1 (red squares), 2 (green diamonds), 4 (black circles) or 6 (blue triangles) hours. The left panels of each set show the dose-response of parasite viability for each exposure time examined. The right panels of each set show viability as a function of the cumulative effective dose for each exposure time examined. The curves correspond to the best fits obtained using the cumulative effective dose model (Eq. S2.4) with the parameters shown in Table 1. The ring data in (B) and (F) are also reproduced in Fig. 3A and 5A.

S3. Simulation of *in vitro* assays: influence of model parameters on $LD_{50}(t^e)$ and $V_{min}(t^e)$

Two useful parameters that can be readily obtained from *in vitro* drug assays are the $LD_{50}(t^e)$ value for the entire parasite population and the fraction of the parasite population that resists high drug concentrations. We define the latter population in terms of the minimum parasite viability (V_{min}) measured at high drug concentrations ($C >> K_m$). Hence, from Eq. S2.4:

$$V_{\min}(t^e) = \left[1 + \left(\frac{t^e}{t_{50}^{e,sat}}\right)^{\gamma}\right]^{-1} \quad \text{[S3.1]}$$

The dependence of LD_{50} on t^e can also be derived from Eq. S2.4:

$$LD_{50}(t^e) = \frac{t_{50}^{e,sat} K_m}{t^e - t_{50}^{e,sat}} \quad \text{[S3.2]}$$

We examined the influence of each of the model parameters (γ, K_m and $t_{50}^{e,sat}$) on $LD_{50}(t^e)$ and $V_{min}(t^e)$ values using the parameters obtained from the DHA treatment of 3D7 rings (Table 1) as a reference point. Each individual parameter was varied to cover the typical range of parameter values observed experimentally while the other parameters were held constant. Simulations were performed for 3, 6 and 24 h of drug exposure (Fig. S3).

$LD_{50}(t^e)$ is independent of γ (Eq. S3.2), but $V_{min}(t^e)$ is strongly influenced by γ (Eq. S3.1, Fig. S3A). The $V_{min}(t^e)$ values exhibit approximate exponential decays with respect to γ with the magnitude of the change in γ associated with a halving of $V_{min}(t^e)$ strongly dependant on t^e (change of 2.3 and 0.7 in γfor pulses of 3 and 6 h of drug exposure, respectively). That is the V_{min} value doubles with every 2.3 and 0.7 decrease in γ, respectively.

While by definition (we are considering $C >> K_m$), $V_{min}(t^e)$ is independent of K_m (Eq. 3.1); the magnitude of K_m does influence $LD_{50}(t^e)$ (Eq. S3.2, fig. S3B). $LD_{50}(t^e)$ is directly proportional to K_m so that while the absolute $LD_{50}(t^e)$ values change in response to K_m, the ratio of $LD_{50}(t^e)$ values measured at different exposure times is unaltered.

The magnitude of $t_{50}^{e,sat}$ has large effects on both $LD_{50}(t^e)$ and $V_{min}(t^e)$ values. Its effect on LD_{50} values is highly dependent on t^e so that small changes in $t_{50}^{e,sat}$ result in large changes to the ratio of LD_{50} values measured with 3 and 6 h drug exposures (Fig. S3D). $V_{min}(t^e)$ values are also heavily influenced by $t_{50}^{e,sat}$. As expected, $V_{min}(t^e)$ values increase sharply as the magnitude of $t_{50}^{e,sat}$ approaches the length of the assay (Fig. S3E).

In summary, this analysis demonstrates that *in vitro* assays employing 3 and 6 h drug exposures of ring stage parasites are suitable for identifying strain-specific responses to the clinically relevant drug, DHA. Of particular note is the observation that the $LD_{50}(t^e)$ value alone may be insufficient to classify a strain as resistant or sensitive necessitating the determination of $V_{min}(t^e)$ values.

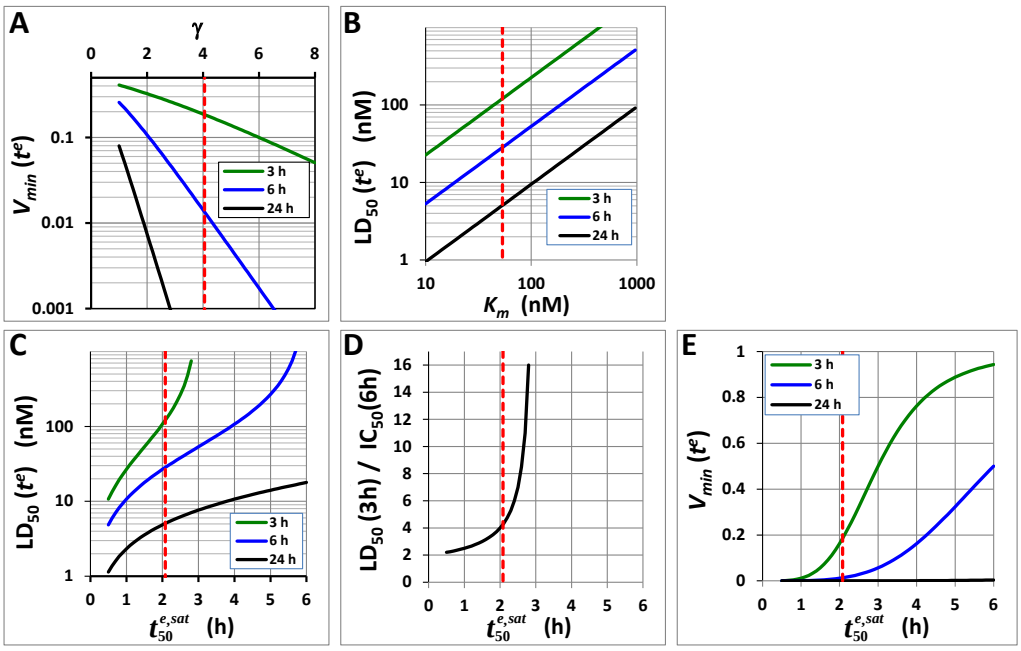

Fig. S3. Simulation of the influence of various model parameters on the magnitude of $LD_{50}(t^e)$ and $V_{min}(t^e)$ values from *in vitro* drug assays. $LD_{50}(t^e)$ and $V_{min}(t^e)$ values were simulated using Eq. S2.4 and the γ, K_m and $t_{50}^{e,sat}$ parameters determined from the DHA treatment of 3D7 ring stage parasites (Table 1) as described in section S3. Each individual parameter was varied to cover the typical range of values observed experimentally while the other parameters were kept constant. The value of the parameter for DHA in ring stage parasites is indicated by the vertical red line. The simulation was performed for drug exposure times of 3, 6 and 24 h. Shown are the effects of γ on $V_{min}(t^e)$ (A), K_m on $LD_{50}(t^e)$ (B), and $t_{50}^{e,sat}$ on $LD_{50}(t^e)$ (C) and $V_{min}(t^e)$ (E). Also shown is the sensitivity of the LD_{50} ratio measured with 3 and 6 h drug exposures on the $t_{50}^{e,sat}$ value (D).

S4. Simulation of a single dose treatment of 3D7 ring-stage parasites (Fig. 5B,C)

Parasites *in vivo* are exposed to fluctuating drug concentrations and varying lengths of drug exposure during endoperoxide chemotherapy. We attempted to mimic these *in vivo* conditions by simulating a DHA profile from a one-compartment PK model with first order absorption and elimination (C_{max} 3 μM, absorption half-life 0.2 h and elimination half-life 1 h) and allowing C in Eq. S2.1 to follow this profile, i.e. $C = C(t)$. The cumulative effective dose is then given by:

$$ED^{cum}(t^e) = \int_0^{t^e} ED(t)dt = ED^{max}\int_0^{t^e}\left(\frac{C(t)}{K_m + C(t)}\right)dt \qquad [S4.1]$$

Note that if C is independent of time, we recover $ED^{cum}=ED^{max}(C/K_m+C)t^e$ as presented in the main text and used for the analysis of our *in vitro* data.

For time-varying $C=C(t)$, Eq. S4.1 must be integrated numerically, and the result fed into Eqs. S2.2 –S2.4 to determine viability as a function of exposure time, t^e:

$$V(C,t^e) = \left[1+\left(\frac{\int_0^{t^e}\left(\frac{C(t)}{K_m + C(t)}\right)dt}{t_{50}^{e,sat}}\right)^{\gamma}\right]^{-1} \qquad [S4.2]$$

We evaluated Eq. S4.2 under these anticipated *in vivo* drug conditions with model parameters set to the estimates presented in Table 1 for 3D7 ring stage parasites treated with DHA. The purpose of this simulation was to examine parasite viability during the course of a DHA pulse with a profile similar to that which would be expected following a single course of drug treatment.

The simulated viability profile of these parasites is shown in Fig. 5B. Two useful parameters that can be extracted from such a viability profile are the time it takes to kill 50% of the parasites (t_{50}^e) and the fraction of parasites that survive the drug pulse (the residual viability, V_{res}). These parameters have values of 2.2 h and 1%, respectively, in this example.

We next examined how drug stability will affect t_{50}^{e} and V_{res} values. Drug stability was altered by changing the elimination half-life, $t_{½}$, of the drug. Altering the stability has little effect on t_{50}^{e} (Fig. S4A, top panel) because drug concentrations remain at saturable levels ($C >> K_m$= 53 nM) for a sufficient time to kill 50% of the parasites at the maximum rate (*i.e.* $t_{50}^{e} \approx t_{50}^{e,sat}$ =2.05 h) even at the shortest drug half-lives values examined. In contrast V_{res} decays exponentially with respect to drug half-life (Fig. S4A, bottom panel) so that V_{res} decreases by 50% for every 0.3 h increase in drug half-life. This demonstrates that relatively small improvements in drug stability can have profound effects on the number of parasites surviving treatment.

We then examined the influence of the various model parameters (γ, K_m and $t_{50}^{e,sat}$) on the t_{50}^{e} and V_{res} values. Using the parameters obtained from the DHA treatment of 3D7 rings (Table 1) as a reference point, each individual parameter was varied to cover the typical range of parameter values observed experimentally while the other parameters were held constant.

K_m values <100 nM have only a small influence on t_{50}^{e} values which are approximately equivalent to $t_{50}^{e,sat}$ (Fig. S4B, top panel). The t_{50}^{e} value increases with larger K_m values because the drug concentrations achieved during the pulse approach the K_m so the system is no longer under conditions of saturating drug concentration. In contrast, the relationship between K_m and V_{res} remains approximately linear across the K_m values examined (Fig. S4B, lower panel). Note that this is not inconsistent with the analysis in section S3, as our assumption $C >> K_m$ is no longer satisfied.

The value of γ has no effect on t_{50}^{e} but has large effects on V_{res} (Fig. S4C). V_{res} decays exponentially with γ, exhibiting a 2-fold increase with every 0.6 decrease in the γ value. This demonstrates that small decreases in the value of γ may not affect the time it takes to kill 50% of the parasites but can lead to large increases in the number of parasites surviving a drug pulse with a clinically relevant profile.

The t_{50}^{e} value is approximately equivalent to the value of $t_{50}^{e,sat}$ until the latter approaches ~ 6 h (Fig. S4D, top panel). The V_{res} values are also strongly influenced by the $t_{50}^{e,sat}$ parameter. The relationship between these parameters is approximated by the relationship: $V_{res} = (t_{50}^{e,sat})^{3.8}$. With respect to the V_{res} value determined in rings (vertical dashed line in Fig. S4D, bottom panel), a 20% increase in $t_{50}^{e,sat}$ approximately doubles V_{res}.

In summary, this analysis demonstrates that relatively small changes in the drug-parasite interaction, as exemplified by the model parameters, can lead to substantial increases in the number of parasites that survive a drug pulse with a clinically relevant profile. Importantly, this analysis demonstrates that a parameter like t_{50}^{e} which measures the time it takes to kill the bulk of the parasite population, is not always a reliable predictor of the fraction of the parasite population that can survive such a treatment.

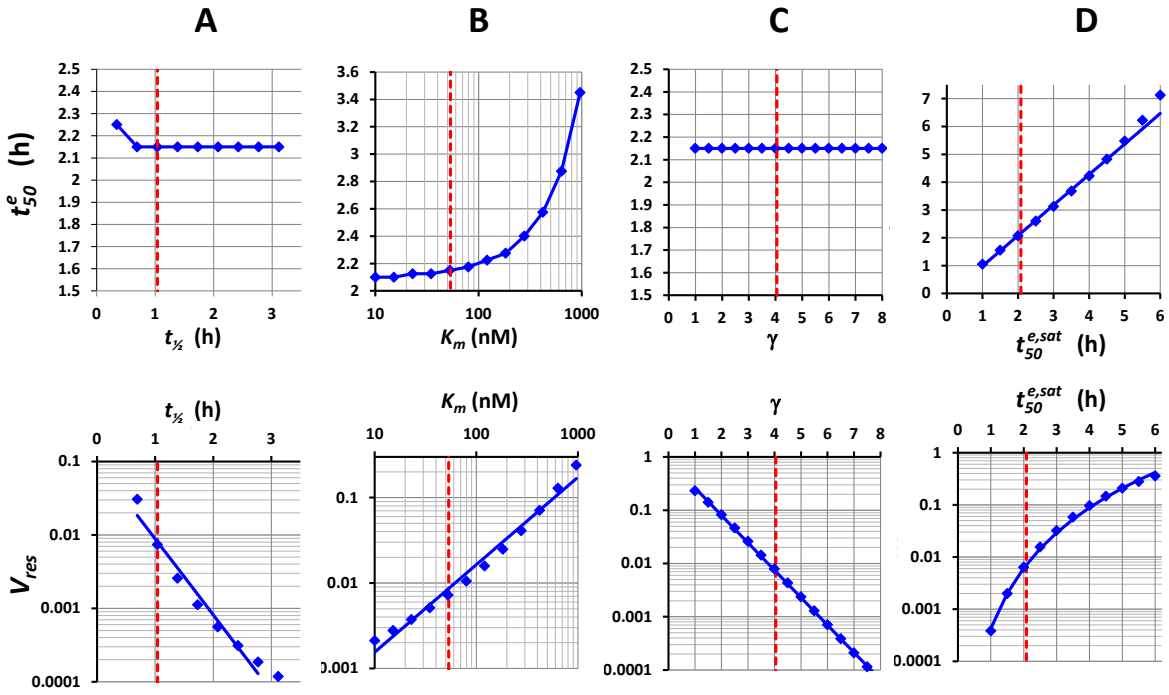

Fig. S4. Simulation of the influence of drug stability (A) and various model parameters (B-D) on t_{50}^{e} and V_{res} values for parasites subjected to an *in vivo*-like DHA pulse. Simulations were carried out as described in section S4 using a drug elimination half-life of 1 h and the parameters obtained from DHA treatment of 3D7 ring stage parameters (Table 1) as reference points. The reference values for these parameters are indicated by the vertical broken red line in each of the figures.

S5. Simulation of a multi dose treatment (D10 and 7G8 parasites)

Tightly synchronized cultures of D10 and 7G8 parasites were subjected to DHA pulses of various durations at ring and trophozoite stages (14 and 28 h p.i., respectively; Fig. S5A) and the viability data analyzed according to the cumulative effective dose model (Fig S5B). The resultant model parameters were used to simulate parasite clearance during the course of a 3-day drug treatment regimen (Fig. S5C) as described in the figure caption.

A

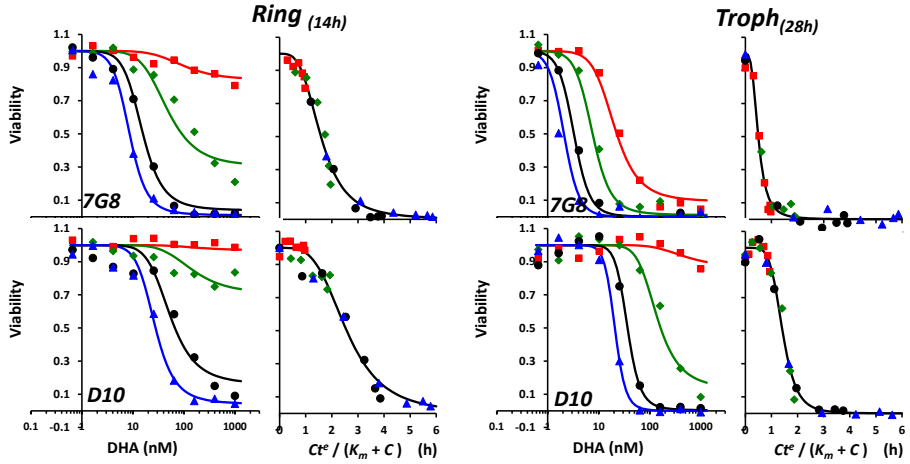

B

Strain	Stage	Parameter		
		K_m (nM)	$t_{50}^{n,x\omega}$ (h)	γ
7G8	$Ring_{(14h)}$	24	1.6	3.4
	$Troph_{(28h)}$	23	0.5	3.2
D10	$Ring_{(14h)}$	37	2.6	3.7
	$Troph_{(28h)}$	67	1.4	5.4

C

Time (h)	Drug Treatment	Parasite Cycle	Parasite Stage	Relative Parasitemia (%) 7G8	D10	Ratio (D10/7G8)
0	#1	1	$Ring_{(14h)}$	100	100	
24	#2	1	$Troph_{(38h)}$	0.35	1.87	5.3
48	#3	2	$Ring_{(14h)}$	0.41×10^{-3}	4.2×10^{-3}	10.2
72		2	$Troph_{(38h)}$	0.14×10^{-5}	7.9×10^{-5}	54.7

Fig. S5. Simulation of parasite clearance of D10 and 7G8 parasites during a 3 day DHA treatment. (A) Dependence of parasite viability (D10 and 7G8 strains) on DHA concentration, DHA exposure time and the cumulative effective dose at mid-ring and mid-trophozoite stage. The average ages of the parasites at the beginning of the assays were 14 and 28 h p.i., respectively. Symbols as in Fig. S2. The curves correspond to the best fits obtained using the cumulative effective dose model (Eq. S2.4) with the parameters shown in (B). (C) Simulation of parasite clearance during the course of a 3-day drug treatment regimen. The parasites are assumed to be mid-rings (14 h p.i.) at the start of treatment, to exhibit 48 h lifecycles, and to undergo a 10-fold multiplication rate between cycles. The simulation also assumes that the parasites remain tightly synchronized so that the 3 drug treatments are administered at mid-ring, trophozoite and mid-ring stages, respectively. The parasite load at each time point was calculated as described in section S4 based on the parasite stage during the previous treatment using the model parameters for the appropriate stage and the DHA pharmacokinetic profile shown in Fig. 5b.

S6. Stage-dependence of parasite sensitivity to QHS, chloroquine and quinine

We examined the stage-dependance of parasite senisitivty to the quinoline drug chloroquine and quinine (Fig. S6). These results show that trophozoites are sensitive to 3 h pulses of chloroquine and quinine but ring stage parasites are insensitive to these drugs for drug pulse durations of at least 6 h. The hRings are also insensitive to chloroquine and quinine indicating that the hypersensitivity is specific to the artemisinin class of drugs.

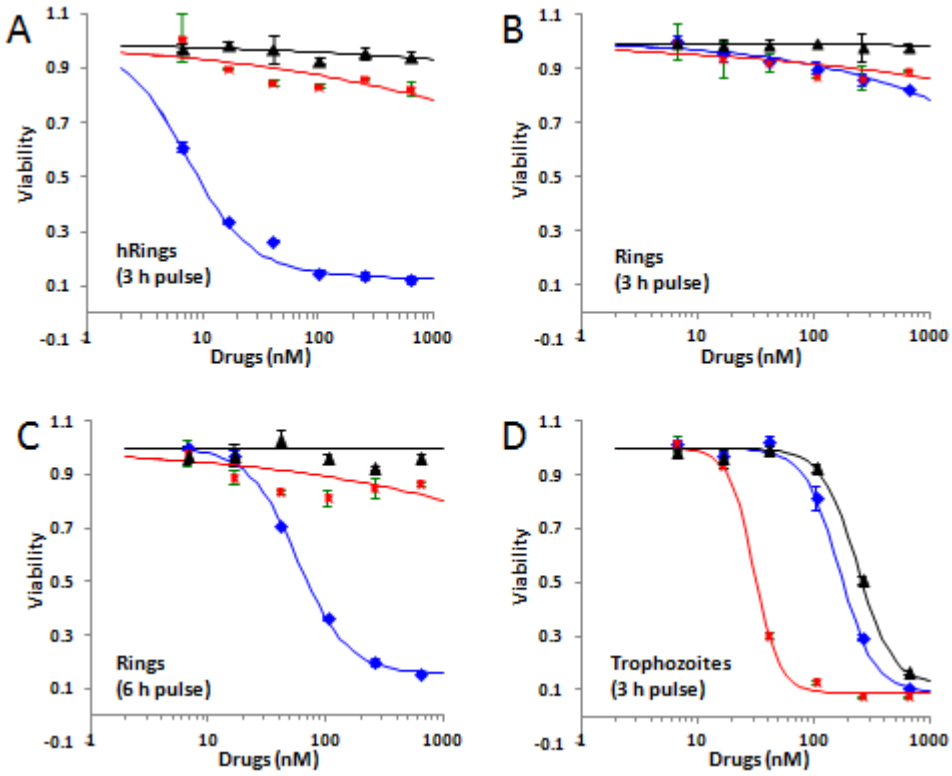

Fig. S6. Stage-dependence of parasite sensitivity to QHS, chloroquine and quinine (blue, red and black symbols, respectively). Tightly synchronized parasite cultures (3D7 strain) consisting of hRings (A), rings (B, C) and trophozoites (D) were subjected to drug pulses of 3 or 6 h durations (as indicated on figure). The parasite ages were 1.5, 7 and 24 h p.i., respectively, at the commencement of the drug pulses. Error bars correspond to the range of duplicates.

Table S1. Correlation coefficients between the parameter estimates shown in Table 1.

Stage	Correlation Coefficient					
	QHS			DHA		
	K_m, $t_{50}^{e,sat}$	K_m, γ	γ, $t_{50}^{e,sat}$	K_m, $t_{50}^{e,sat}$	K_m, γ	γ, $t_{50}^{e,sat}$
hRing (2h)	0.60	-0.58	-0.93	0.35	-0.36	-0.83
Ring (7.5h)	-0.03	-0.08	-0.71	0.10	-0.26	-0.64
Troph (24h)	0.51	-0.49	-0.95	0.19	-0.27	-0.8
Troph (34h)	0.39	-0.38	-0.92	0.25	-0.21	-0.85

K_m - Drug concentration resulting in half the maximum effective dose.

$t_{50}^{e,sat}$ - Exposure time required for 50% parasite killing at saturating drug concentrations.

γ - Slope of the sigmoidal function relating parasite viability and cumulative ED.